arXiv:1611.02206v1 [math-ph] 7 Nov 2016

GROUP THEORETICAL METHODS TO CONSTRUCT THE GRAPHENE

Z. GRABOWIECKA[2,3], J. PATERA[1,2,3], AND M. SZAJEWSKA[4,1]

Abstract. In this paper, the tiling of the Euclidean plane with regular hexagons is called a graphene. The vertices of the hexagons are carbon atoms. We describe six different ways to generate the graphene. There are two ways starting from the triangular lattice of A_2, and one way for each algebra G_2, B_3, C_3 and A_3, by projecting the weight system of their lowest representation to the hexagons of A_2. Colouring of the graphene is presented. Changing from one colouring to another is called phase transition. For a fixed number of colours of the graphene, phase transition transformations form a finite Abelian group. Multistep refinements of the graphene are described.

[1] MIND Research Institute, 111 Academy Drive, Irvine, CA 92617
[2] Centre de recherches mathématiques, Université de Montréal, C. P. 6128, succ. Centre-ville, Montréal, H3C 3J7, Québec, Canada
[3] Département de mathématiques et de statistique, Université de Montréal, C. P. 6128, Centre-ville, Montréal, H3C 3J7, Québec, Canada
[4] Institute of Mathematics, University of Bialystok, 1M Ciolkowskiego, PL-15-245, Bialystok, Poland

E-mail: zofia.grabowiecka@gmail.com, patera@crm.umontreal.ca, m.szajewska@math.uwb.edu.pl

1. Introduction

The simplest prescription for forming a graphene sheet is to take a regular hexagon and to reflect it an unlimited number of times in its sides. This is a simple construction, which offers no insight as to which structures the hexagon originated from. In view of the very interesting physical properties of the graphene, where the vertices of hexagons are populated by carbon atoms [7, 9], one is motivated to look for the structures from which the original hexagon arose.

In this paper, we use group theory to describe six different ways to obtain such a hexagon. They are related to the reflection groups associated with simple Lie groups $SU(3)$, $O(6)$, $O(7)$, $G(2)$, $Sp(6)$. Throughout the paper, we use the notation standard for Lie algebras rather than Lie groups, namely, $SU(3)$ is replaced by A_2, $G(2)$ by G_2, $O(6)$ by A_3, $O(7)$ by B_3, and $Sp(6)$ by C_3.

Distinguished among these possibilities is the pair of cases with A_2 and G_2 symmetries. A graphene constructed according to one of the two symmetries can be transformed into a graphene constructed with the other symmetry by inverting the corresponding projection matrix. Both graphenes are isomorphic. First, the A_3, C_3 and B_3 cases are used to produce their hexagons, which are in 3-dimensional space and not in a plane. Then, the projection matrices are provided that transform them into planar hexagons.

The tool that allows us to consider all these cases in parallel is the projection matrix from the root space of the algebra G to the root space of its subalgebra G' [12, 14, 15]. In all cases, corresponding bases are called ω-bases. Geometrically, these bases are given here in terms of 2×2 or 3×3 matrices for each case separately (see Appendix). Since we are projecting the orbits of the reflection groups resulting in one or several orbits of the smaller reflection group, the projection matrices listed in the text are not unique. Indeed, the orbits are invariant with respect to the reflection group of G on one hand, and the reflection group of G' on the other. Therefore, the projection matrices may be modified by the transformation of Weyl groups of G into G'.

The projection matrices used here were calculated for the computation of branching rules [15] and published in [12]. They were optimized for the large scale machine computation of branching rules.

2. Construction of the graphene sheet

2.1. Lie algebra A_2 and the graphene.

There are two ways to construct the graphene sheet from the triangular lattice of Lie algebra A_2. There are two lattices corresponding to A_2, namely root lattice Q and weight lattice P. Each point of Q is of the form $\mathbb{Z}\alpha_1+\mathbb{Z}\alpha_2$, where α_1, α_2 are simple roots of Lie algebra A_2 and $\mathbb{Z}$ are any integers. They are of the same length, the angle between them is $2\pi/3$, and they form the so-called α-basis. Points of the weight lattice P are of the form $\mathbb{Z}\omega_1 + \mathbb{Z}\omega_2$, where ω_1, ω_2 are weights of A_2 forming the ω-basis, and $\mathbb{Z}$ are any integers. The correspondence between α- and ω-bases is given by the Cartan matrix and its inverse [5, 10]. In the case of Lie algebra A_2, the matrix is of the form $C = \begin{pmatrix} 2 & -1 \\ -1 & 2 \end{pmatrix}$, its inverse is $C^{-1} = \frac{1}{3}\begin{pmatrix} 2 & 1 \\ 1 & 2 \end{pmatrix}$ and then

$$\alpha_1 = 2\omega_1 - \omega_2, \quad \alpha_2 = -\omega_2 + 2\omega_2, \quad \omega_1 = \frac{2}{3}\alpha_1 + \frac{1}{3}\alpha_2, \quad \omega_2 = \frac{1}{3}\alpha_1 + \frac{2}{3}\omega_2.$$

In the first method, the graphene sheet is formed by the Brillouin zones of the points of root lattice Q. The Brillouin zone is also called proximity cell, or in physics literature, *Wigner-Seitz cell* or *Voronoi domain* [13].

In other words, the graphene sheet is obtained by assigning to every point of Q its Brillouin zone, that is, the area closer to a given point of Q than to any other point of Q. Every Brillouin zone of a point of Q is a regular hexagon. Preserving the hexagons and removing the points of the root lattice from the centers of the hexagons yields the graphene sheet. The Brillouin zones for lattices of all simple roots were described in [13].

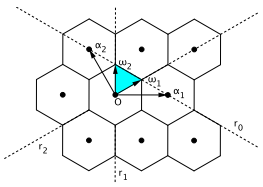

Figure 1. Fragment of the Q lattice of A_2 where the Brillouin zones are shown.

In the second method, we define three congruence classes of points of weight lattice P. Point $a\omega_1 + b\omega_2$ belongs to one of the three congruence classes according to $a + 2b \mod 3$.

The triangular lattice is the union of the points of the three congruence classes $K_i = \{a + 2b \equiv i \mod 3\}, i = 0, 1, 2$. Points of the congruence class K_0 coincide with the root lattice Q, points of K_1 are formed as $\omega_1 + Q$, points of K_2 are formed as $\omega_2 + Q$. The vertices of the hexagons forming the graphene sheet are obtained by removing from P points of the congruence class K_0. Each hexagon of the graphene has three vertices in the congruence class K_1 and three vertices in the congruence class K_2 (see Fig. 2). The origin of the graphene sheet is chosen as the center of one of the hexagons. The center clearly belongs to congruence class K_0.

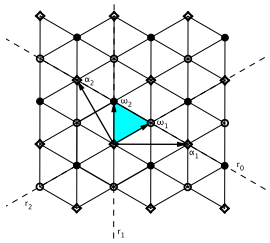

FIGURE 2. Fragment of the P lattice of A_2 is shown. Points of congruence class K_1 are marked by circles, points of congruence class K_2 are marked by black dots, and points of congruence class K_0 are marked by rectangles.

More generally one can remove any one of the three congruence classes and remaining set of points will be a graphene.

2.2. **Reflections generating the affine Weyl group of A_2.**

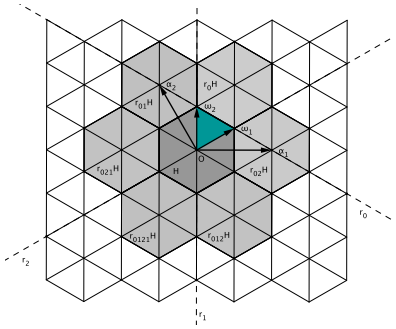

FIGURE 3. Hexagon H and its neighbours, each shown with the reflections used to obtain them. Notation $r_{ij}H$ shows the reflections needed to get the hexagon. First, we apply r_i, then r_j to H.

Let α_1 and α_2 be simple roots of A_2. The highest root of A_2 is $\alpha_0 = \alpha_1 + \alpha_2$. The reflections in planes orthogonal to the simple roots are given

by the formula

$$r_i(x) = x - \frac{2(x,\alpha_i)}{(\alpha_i,\alpha_i)}\alpha_i, \quad i = 1,2 \tag{1}$$

where $(\cdot,\cdot)$ is a scalar product, and x is any point in the Euclidean plane. Reflections r_1, r_2 generate the Weyl group of A_2, which is of order 6. When the affine reflection

$$r_0(x) = \alpha_0 + x - \frac{2(x,\alpha_0)}{(\alpha_0,\alpha_0)}\alpha_0 \tag{2}$$

is included, the affine Weyl group is of infinite order.

2.3. **Simple Lie algebra G_2 and the graphene.**

The subsequent four cases described in this paper are formed as follows. We look for Lie algebras where A_2 is maximal. Their lowest representation contains the hexagonal orbit of weights, which is subsequently projected by known projection matrices into the hexagons of A_2. Each hexagon is then reflected in its sides by the affine Weyl group of A_2, so that it is spread all over the plane, forming the graphene. The only exception is the chain of subalgebras $B_3 \supset G_2 \supset A_2$, where G_2 is maximal in B_3 and A_2 is maximal in G_2. This is the exceptional inclusion of G_2, which has analogs only in much higher ranks of Lie algebras [8]. The exceptional position of G_2 was noted years ago by Racah [17].

Consider the case of the G_2 algebra. Starting from the irreducible 7 dimensional representation of G_2, which is the lowest representation of dimension > 1, the representation of G_2 can be reduced to the direct sum of three representations of A_2. The reduction process from G_2 to A_2 consists of projecting the weights of G_2 representation into weights of A_2 representations. This is an orthogonal projection provided by 2×2 matrix found in [12], namely

$$Pr(G_2 \to A_2) = \begin{pmatrix} 1 & 1 \\ 1 & 0 \end{pmatrix}. \tag{3}$$

The result of the projection are two triangular orbits of A_2, and the origin, which is an orbit in itself, see Example 1. Making the centers of A_2 triangles coincide, we obtain a regular hexagon, plus the center point. Removing the center point, we have a hexagon, which, by repeated reflections of the affine Weyl group, gives us the graphene. The projection is done for the G_2 weights, which are written in the ω-basis of G_2, namely

$$\{(0,1),(1,-1),(-1,2),(1,-2),(-1,1),(0,-1)\} \tag{4}$$

and result is in the ω-basis of A_2.

Example 1. *Let us apply the projection matrix* (3) *to the lowest non-trivial G_2 orbit* (4) *(orbit of the lowest dominant weight). The projection matrix $Pr(G_2 \to A_2)$ applied to the weight* $(0,1)$ *of G_2 is equal to*

$$\begin{pmatrix} 1 & 1 \\ 1 & 0 \end{pmatrix} \begin{pmatrix} 0 \\ 1 \end{pmatrix} = \begin{pmatrix} 1 \\ 0 \end{pmatrix}$$

weight of A_2. Similarly, we project the remaining weights of the orbit points

$$\left(\begin{smallmatrix} 1 & 1 \\ 1 & 0 \end{smallmatrix}\right) \left(\begin{smallmatrix} 1 \\ -1 \end{smallmatrix}\right) = \left(\begin{smallmatrix} 0 \\ 1 \end{smallmatrix}\right),$$
$$\left(\begin{smallmatrix} 1 & 1 \\ 1 & 0 \end{smallmatrix}\right) \left(\begin{smallmatrix} -1 \\ 2 \end{smallmatrix}\right) = \left(\begin{smallmatrix} 1 \\ -1 \end{smallmatrix}\right),$$

$$\begin{pmatrix}1&1\\1&0\end{pmatrix}\begin{pmatrix}1\\-2\end{pmatrix}=\begin{pmatrix}-1\\1\end{pmatrix},$$
$$\begin{pmatrix}1&1\\1&0\end{pmatrix}\begin{pmatrix}-1\\1\end{pmatrix}=\begin{pmatrix}0\\-1\end{pmatrix},$$
$$\begin{pmatrix}1&1\\1&0\end{pmatrix}\begin{pmatrix}0\\-1\end{pmatrix}=\begin{pmatrix}-1\\0\end{pmatrix}.$$

The result of the projection are the six vertices of the A_2 hexagon. Note, however, that this hexagon is formed by two triangular orbits centered at the origin, namely $\{(1,0),\ (-1,1),\ (0,-1)\}$ and $\{(0,1),\ (1,-1),\ (-1,0)\}$.

It may be useful in some future applications to notice that the projection matrix (3) is invertible. Therefore, the A_2 graphene can be projected into the set of points of G_2, which form the G_2 graphene.

2.4. **3-dimensional hexagons and the graphene.**
The graphene can be produced starting from the 3-dimensional hexagons arising from rank 3 Lie algebras A_3, B_3 and C_3. Subsequently, projecting non-planar hexagons (Fig. 4) to planar hexagons, and then reflecting them by the affine Weyl group of A_2, we obtain the graphene sheet.

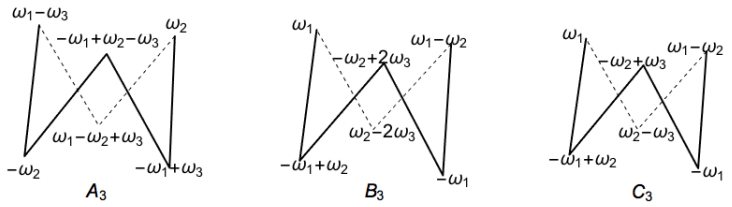

FIGURE 4. Nonplanar hexagons with vertices in the coordinates of ω-bases of A_3, B_3 and C_3.

Curiously, the 3 hexagons in 3-dimensions, A_3, B_3 and C_3, are identical as geometric structures. Their vertices are labelled in 3 different ω-bases, as shown in Fig. 4

Consider the weight system of the irreducible representation of A_3 with the highest weight $(0,1,0)$ in A_3 ω-basis. The three reflections in the hyperplane orthogonal to the simple roots of A_3, and intersecting in the origin applied to the highest weight, yield the hexagon with vertices

$$\{(0,1,0),(1,-1,1),(1,0,-1),(0,-1,0),(-1,1,-1),(-1,0,1)\}. \tag{5}$$

The projection matrix

$$Pr(A_3\to A_2)=\begin{pmatrix}1&1&0\\0&0&1\end{pmatrix} \tag{6}$$

transforms the A_3 hexagon (Fig. 4) into the planar A_2 hexagon in its ω-basis, namely

$$\{(1,0),(0,1),(1,-1),(-1,0),(0,-1),(-1,1)\}. \tag{7}$$

The Lie algebra B_3 has the lowest irreducible representation of dimension 7. The weight system of the representation consists of two orbits of the B_3 Weyl group. One orbit of six points forming a hexagon, and one orbit which is the origin. There are two possible chains of maximal subalgebras, which start with B_3 and end in A_2. The first is $B_3\supset G_2\supset A_2$, and the second is

$B_3 \supset A_3 \supset A_2$. The non-planar B_3 hexagon, see Fig. 4, has the following vertices

$$\{(1,0,0),(-1,1,0),(0,-1,2),(-1,0,0),(1,-1,0),(0,1,-2)\} \tag{8}$$

It can be first projected into the G_2 hexagon or into the A_3 hexagon using the appropriate matrix

$$Pr(B_3 \to G_2) = \begin{pmatrix} 0 & 1 & 0 \\ 1 & 0 & 1 \end{pmatrix} \qquad Pr(B_3 \to A_3) = \begin{pmatrix} 0 & 1 & 1 \\ 1 & 0 & 0 \\ 0 & 1 & 0 \end{pmatrix} \tag{9}$$

and then into the A_2 hexagon using either the (3) or (6) matrix. Combining this two-step projection, we get

$$Pr(B_3 \to A_3 \to A_2) = Pr(B_3 \to G_2 \to A_2) = \begin{pmatrix} 1 & 1 & 1 \\ 0 & 1 & 0 \end{pmatrix} \tag{10}$$

In both cases, B_3 to A_2 projection is done using the same matrix. It remains to apply the affine Weyl group of A_2 to obtain the hexagon in order to produce the graphene.

Example 2. *Let us demonstrate the coincidence of the projection matrices of B_3 to A_2 when proceeding with different chains of subalgebras. Consider $B_3 \supset G_2 \supset A_2$. Then*

$$Pr(G_2 \to A_2)Pr(B_3 \to G_2) = \begin{pmatrix} 1 & 1 \\ 1 & 0 \end{pmatrix} \begin{pmatrix} 0 & 1 & 0 \\ 1 & 0 & 1 \end{pmatrix} = \begin{pmatrix} 1 & 1 & 1 \\ 0 & 1 & 0 \end{pmatrix}.$$

Consider $B_3 \supset A_3 \supset A_2$. We get

$$Pr(A_3 \to A_2)Pr(B_3 \to A_3) = \begin{pmatrix} 1 & 1 & 0 \\ 0 & 0 & 1 \end{pmatrix} \begin{pmatrix} 0 & 1 & 1 \\ 1 & 0 & 0 \\ 0 & 1 & 0 \end{pmatrix} = \begin{pmatrix} 1 & 1 & 1 \\ 0 & 1 & 0 \end{pmatrix}.$$

Consider the Lie algebra C_3. Its lowest irreducible representation is of dimension 6. The corresponding weight system consists of six weights

$$\{(1,0,0),(-1,1,0),(0,-1,1),(-1,0,0),(1,-1,0),(0,1,-1)\} \tag{11}$$

in C_3 ω-basis. The orbit forms a non-planar hexagon, see Fig. 4. The projection matrix

$$Pr(C_3 \to A_2) = \begin{pmatrix} 1 & 1 & 2 \\ 0 & 1 & 0 \end{pmatrix} \tag{12}$$

transforms the hexagon of C_3 into the same A_2 hexagon as in the previous cases.

3. Colouring the graphene

In this section, we will introduce another hierarchy of the hexagons in a graphene sheet. We call it *colouring*, for lack of a better name. In addition, we also consider transformations between different colourings, which we refer to as phase transitions. There is an algebraic rule for assigning an integer (colour) to each hexagon. Practically, we proceed as follows. The center of each hexagon is a point of congruence class K_0 of the weight lattice P of A_2. It also happens to be a point of the root lattice Q of A_2. We therefore assign a colour to each point of Q, and recognize that this is the colour of

the whole hexagon containing the point. The number of colours can be any positive integer, but in this paper we focus on 2 and 3 colours in detail.

A point of Q is of the form $a\alpha_1 + b\alpha_2$, where $a, b \in \mathbb{Z}$. The colour of the point is defined as

$$\begin{pmatrix} a & b \end{pmatrix} \begin{pmatrix} k_1 \\ k_2 \end{pmatrix} = k_1 a + k_2 b \mod m, \tag{13}$$

where the positive integer m is the number of colours, and the pair (k_1, k_2) specifies the colouring type. The trivial colouring is given by $(k_1, k_2) = (0, 0)$.

Suppose we have a coloured graphene of the type (k_1, k_2). We can represent the colouring as a column vector $(k_1, k_2, 1)^T$. The transition to another colouring characterized by integers $(l_1, l_2) \mod m$ is given by the matrix

$$T = \begin{pmatrix} 1 & 0 & l_1 \\ 0 & 1 & l_2 \\ 0 & 0 & 1 \end{pmatrix}. \tag{14}$$

Namely,

$$\begin{pmatrix} 1 & 0 & l_1 \\ 0 & 1 & l_2 \\ 0 & 0 & 1 \end{pmatrix} \begin{pmatrix} k_1 \\ k_2 \\ 1 \end{pmatrix} = \begin{pmatrix} k_1 + l_1 \\ k_2 + l_2 \\ 1 \end{pmatrix}. \tag{15}$$

Composition of several transitions is possible, through a product of matrices i.e.,

$$\begin{pmatrix} 1 & 0 & l_1 \\ 0 & 1 & l_2 \\ 0 & 0 & 1 \end{pmatrix} \begin{pmatrix} 1 & 0 & c_1 \\ 0 & 1 & c_2 \\ 0 & 0 & 1 \end{pmatrix} = \begin{pmatrix} 1 & 0 & l_1 + c_1 \\ 0 & 1 & l_2 + c_2 \\ 0 & 0 & 1 \end{pmatrix} \tag{16}$$

Clearly, for every transition matrix T, there exists its inverse

$$\begin{pmatrix} 1 & 0 & l_1 \\ 0 & 1 & l_2 \\ 0 & 0 & 1 \end{pmatrix} \begin{pmatrix} 1 & 0 & -l_1 \\ 0 & 1 & -l_2 \\ 0 & 0 & 1 \end{pmatrix} = \begin{pmatrix} 1 & 0 & 0 \\ 0 & 1 & 0 \\ 0 & 0 & 1 \end{pmatrix}$$

Therefore, the phase transition matrices T form a finite Abelian group whose order is controlled by the number of colours m.

3.1. **2-colourings of the graphene.**

There are 3 non-equivalent ways to assign 2 colours to all the points of Q. In other words, there are 3 different non-trivial 2-colourings of the graphene sheet. Namely,

$$(k_1, k_2) = (1, 0), \qquad (k_1, k_2) = (0, 1), \qquad (k_1, k_2) = (1, 1).$$

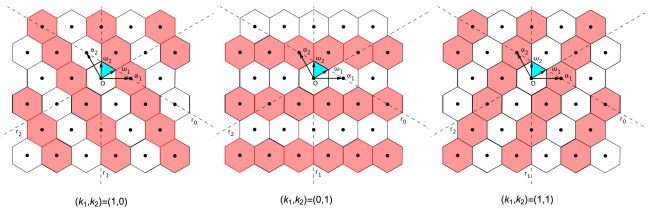

FIGURE 5. Examples of fractions of the graphene with 2-colouring of the hexagons.

Any other choice of integers (k_1, k_2) turns out to be equivalent to one of the given three, because we are considering the colouring mod 2. Examples of the three types of such colouring are shown in Fig. 5.

3.2. **3-colourings of the graphene.**

There are 8 non-trivial choices of integers (k_1, k_2) mod 3 that specify non-equivalent 3-colourings of the graphene's hexagons. These are the following:

$$(k_1, k_2) = (1, 0), \quad (k_1, k_2) = (0, 1), \quad (k_1, k_2) = (1, 1),$$
$$(k_1, k_2) = (2, 0), \quad (k_1, k_2) = (0, 2), \quad (k_1, k_2) = (2, 2),$$
$$(k_1, k_2) = (1, 2), \quad (k_1, k_2) = (2, 1).$$

Examples of such colourings are shown in Fig 6.

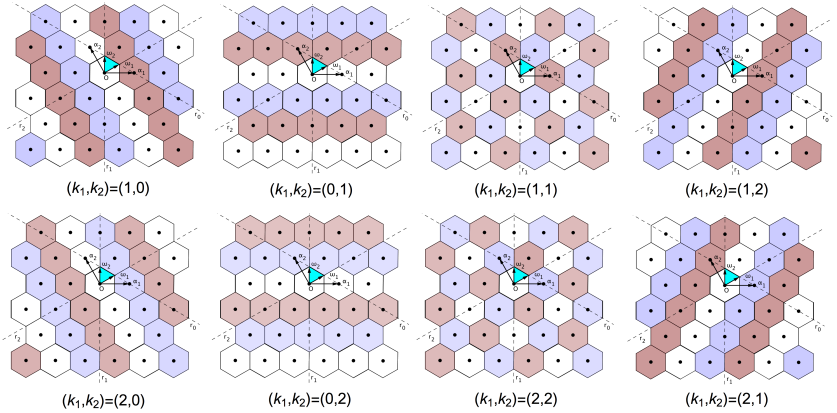

FIGURE 6. Examples of fractions of the graphene with 3-colouring of hexagons.

Analogously, colouring can be done for an arbitrary $m < \infty$.

4. Refinement of the graphene

A primitive and straightforward way to refine the graphene is to cut each of its hexagons into smaller hexagons. In this case, admissible sizes of these hexagons must be set. In the paper, we present two more systematic ways to refine the graphene.

Consider the graphene and the vertices of each hexagon. Brillouin zones (proximity cells) of the vertices of hexagons form a triangular lattice P' in $\mathbb{R}^2$. These triangles are smaller than those in the original weight lattice P of A_2. Three congruence classes of points of P' can be defined. The graphene of P' is obtained by deleting the congruence class zero from the lattice P'. This process can be repeated as many times as desired, creating a graphene of smaller and smaller hexagons at each step.

The second method is more powerful, as well as more general. In this paper, it is only used for the Lie algebra A_2. The refinement of the graphene starts with the refinement of the lattice P of A_2. The basic tile F in the lattice P is the coloured triangle in Fig. 2. Its vertices are $0, \omega_1, \omega_2$. Fix a positive integer M. We obtain $|F_M(A_2)| = \binom{M+2}{2}$ points in the basic

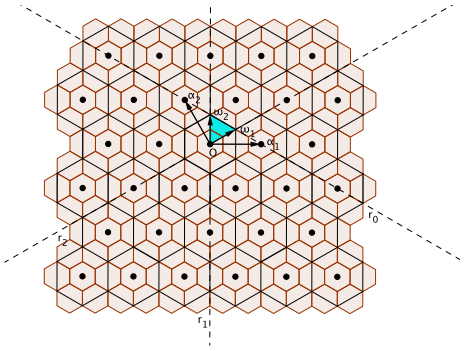

FIGURE 7. Fragment of the refinement of a graphene sheet.

tile and on its boundary, by providing the 3 nonnegative integers $[s_0, s_1, s_2]$ such that

$$s_0 + s_1 + s_2 = M. \tag{17}$$

The coordinates of the points in F_M are $\frac{s_1}{M}\omega_1 + \frac{s_2}{M}\omega_2$. When one considers all possible choices for s_i integers such that (17) holds, one obtains the refinement of the basic tile, where the points are vertices of the triangles. Reflections from the affine Weyl group of A_2 spread the refinement onto the whole plane. Taking the refined lattice, we can start to build the graphene as in section 2.1, and obtain a refined graphene whose density is fixed by M.

5. Concluding remarks

Thus far, we have considered the possibility of constructing the A_2 graphene by means of the inclusion of A_2 as a maximal subalgebra of some higher rank algebras. A few additional possibilities exist. Rather than making A_2 a maximal subalgebra of a simple Lie algebra, we can require that A_2 is a maximal subjoint algebra [16].

The method for constructing the graphene sheet can be generalized to more dimensions in a straightforward way. Indeed, generalization of the graphene sheets built using Brillouin zones is possible for any dimension and any symmetry group. The classification of Brillouin zones is found in [13].

Generalization of the construction of graphenes by means of congruence classes is possible only when the symmetry is of type A_n, $n < \infty$. Higher dimensional graphenes are not formed by hexagons in general.

It would be curious to investigate the triangular lattice from the point of view of G_2 symmetry only. The problem is more complicated because the G_2 lattice cannot be decomposed into 3 congruence classes. However, we can use the Brillouin zones to construct the graphene.

Colouring of graphenes can be generalized to higher dimensional lattices of simple Lie algebras. Moreover, the phase transition can be generalized to more dimensions.

It would be interesting to describe finite Abelian groups formed by the phase transitions matrices for more general setups.

Possibilities of colouring the graphene aperiodically remain unexplored. The simplest way to achieve this would be to map Q to the 2-dimensional quasicrystal.

Many properties of the graphene, including colouring, can be extended to nanotubes, which are strips of the graphene of appropriate width, rolled into a cylinder [6, 11]. Different nanotubes are obtained by different orientations of the strips [1–4].

6. Appendix
ω-bases for the Lie algebras and Lie groups considered in this paper

In all cases, we use the ω-basis. The basis vectors are not orthogonal, and sometimes not of the same length. They are derived from the general properties of semisimple Lie groups and algebras. Because they are found in many places, we do not rederive them here, but only recall them. Here, an ω-basis is defined using the scalar product of the basis vectors $\langle\omega_i|\omega_j\rangle$. Therefore, we provide the appropriate matrices of the scalar products.

$$\text{For } A_1\times A_1: \quad \tfrac{1}{2}\begin{pmatrix}1&0\\0&1\end{pmatrix};$$

$$\text{For } A_2: \quad \frac{1}{3}\begin{pmatrix}2&1\\1&2\end{pmatrix};$$

$$\text{For } G_2: \quad \frac{1}{3}\begin{pmatrix}6&3\\3&2\end{pmatrix};$$

$$\text{For } A_3: \quad \frac{1}{4}\begin{pmatrix}3&2&1\\2&4&2\\1&2&3\end{pmatrix};$$

$$\text{For } B_3: \quad \begin{pmatrix}1&1&1\\1&2&2\\1&2&3\end{pmatrix};$$

$$\text{For } C_3: \quad \frac{1}{2}\begin{pmatrix}1&1&1\\1&2&2\\1&2&3\end{pmatrix}.$$

Acknowledgements. Authors are grateful to Dr. Alexandra Patera for stimulating comments and editorial assistance, and to the Natural Sciences and Engineering Research Council of Canada, RGPIN-2016-04199, and the MIND Research Institute of Irvine, California, for partial support of the work.

All authors contributed equally to the paper.

References

[1] M. Bodner, J. Patera and M. Szajewska, *C_{70}, C_{80}, C_{90} and carbon nanotubes by breaking of the icosahedral symmetry of C_{60}*. Acta Cryst. A **69**(6), 583-591, (2013).

[2] M. Bodner, J. Patera and M. Szajewska, *Breaking of icosahedral symmetry: C_{60} to C_{70}*. PLOS ONE **9** (3): e84079, (2014), 10.1371/journal.pone.0084079.

[3] M. Bodner, E. Bourret, J. Patera and M. Szajewska, *Icosahedral symmetry breaking: C_{60} to C_{78}, C_{96} and to related nanotubes*. Acta Cryst. A. **70**(6), 650-655, (2014).
[4] M. Bodner, E. Bourret, J. Patera, and M. Szajewska, *Icosahedral symmetry breaking: C_{60} to C_{84}, C_{108} and to related nanotubes*. Acta Cryst. A. **71**(3), 297-300, (2015).
[5] N. Bourbaki, *Groupes et algèbres de Lie*. Chapters IV, V, VI, Hermann, Paris, (1968).
[6] M. Calaresi, M. Quintana P. Rudofl, F. Zerbetto and M. Prato, *Rolling up a Graphene Sheet*. PCCP, **14** ,3447-3453, (2013).
[7] M.S. Dresselhaus, G. Dresselhaus, and P.C. Eklund *Science of Fullerenes and Carbon nanotubes*. San Diego. Academic Press, (1996).
[8] E.B. Dynkin, *Semisimple subalgebras of semisimple Lie algebras*. AMS Trnanslations, Series 2, Vol. **6**, 111–244, (1957).
[9] P.J.F. Harris, *Carbon Nanotubes and Related Structures*. Cambridge University Press, (1999).
[10] J.E. Humphreys, *Reflection Groups and Coxeter Groups*. Cambridge Studies in Advanced Mathematics, **29**Cambridge University Press, Cambridge, Cambridge University Press, (1990).
[11] O.O. Kit, T. Tallinen, L. Mahadevan, J. Timonen and P. Koskinen, *Twisting graphene nanoribbons into carbon nanotubes. Physical Review B*, **85**, 085428, (2012).
[12] W. McKay, J. Patera and D. Sankoff, *The computation of branching rules for representations of semisimple Lie algebras*. Computers in Nonassociative Rings and Algebras, Academic Press, Inc., (1977).
[13] R.V. Moody and J. Patera, *Voronoi and Delaunay cells of root lattices: classification of their faces and facets by Coxeter-Dynkin diagrams*. (dedicated to the memory of H. Zassenhaus), J. Phys. A: Math. Gen. **25** 5089–5134, (1992)..
[14] M. Nesterenko, J. Patera, M. Szajewska and A. Tereszkiewicz *Orthogonal polynomials of compact simple Lie groups: Branching rules for polynomials*. J. Phys. A Math. Theor., 43, no. 495207, 1–27, (2010).
[15] J. Patera and D. Sankoff, *Branching rules for representations of simple Lie algebras*. Presses Université de Montréal, Montréal, (1973), 99 pages.
[16] J. Patera, R.T. Sharp and R. Slansky, *On a new relation between semisimple Lie algebras*. J. Math. Phys., **21**, 2335-2341, (1980).
[17] G. Racah, *Theory of Complex Spectra. IV*. Phys. Rev. **76**, 1352, (1949).